Thermocapillary convection and phase change in welding

Gustav Amberg and Minh Do-Quang
Department of Mechanics, Royal Institute of Technology, Stockholm, Sweden

Received 16 January 2007
Revised 25 May 2007
Accepted 25 May 2007

Abstract

Purpose – In welding there is an intricate coupling between the composition of the material and the shape and depth of the weld pool. In certain materials, the weld pool may not penetrate the material easily, so that it is difficult or impossible to weld, while other seemingly quite similar materials may be well suited for welding. This is due to the convective heat transfer in the melt, where the flow is driven primarily by surface tension gradients. This paper aims to study how surface active agents affect the flow and thus the welding properties by surveying some recent 3D simulations of weld pools.

Design/methodology/approach – Some basic concepts in the modelling of flow in a weld pool are reviewed. The mathematical models for a convecting melt, with a detailed model for the surface tension and the Marangoni stress in the presence of surfactants, are presented. The effect of the sign of the Marangoni coefficient on the flow pattern, and thus, via melting and freezing, on the shape of the weld pool, is discussed.

Findings – It is seen that it is beneficial to have surfactants present at the pool surface, in order to have good penetration. Results from a refined surface tension model that accounts for non-equilibrium redistribution of surfactants are presented. It is seen that the surfactant concentration is significantly modified by the fluid flow. Thereby, the effective surface tension and the Marangoni stresses are altered, and the redistribution of surfactants will affect the penetration depth of the weld pool.

Originality/value – The importance of surfactants for weld pool shapes, and in particular the convective redistribution of surfactants, is clarified.

Keywords Welding, Convection, Phase transformations

Paper type Research paper

1. Introduction

Gas-tungsten-arc (GTA) welding is a widely used method to join materials in manufacturing industries. Nevertheless, the physical processes involved in GTA-welding are highly complex and are not fully understood. One key issue in improving welding technology is to devise methods suitable for new materials, and to predict the welding properties of a new material in detail. This involves for instance a prediction of the depth and width of the molten region (the weld pool), the structure of the material in the junction after the process is complete, and also how the properties of the material influence the choice of the actual welding parameters, i.e. welding current, speed, etc.

The weld pool shape, and thus the penetration, depends to a large extent on the convective and conductive heat transfer in the weld pool. The conduction heat transfer primarily depends on the properties of the plate, whereas the convective heat transfer is determined by the surface tension force, the magnetic force and buoyancy force, etc. It is well established that the convection in the molten pool significantly affects the weld shape (Debroy and David, 1995). Among those flows, the thermocapillary convection was identified as the main driving force. It can affect the shape of the weld pool dramatically. Some early works, (Sahoo *et al.*, 1988; McNallan and Debroy, 1991),

International Journal of Numerical Methods for Heat & Fluid Flow
Vol. 18 No. 3/4, 2008
pp. 378-386

0961-5539
DOI 10.1108/09615530810853637

used assumptions of equilibrium thermodynamics to model how the temperature coefficient of surface tension changes with both temperature and composition of surface-active elements such as oxygen or sulfur.

There has recently been a growing interest in detailed numerical simulations of weld processes (for representative literature see for instance the conferences, Cerjak (2001) and David and Vitek (1993)). Recently Winkler *et al.* (2000), has questioned the equilibrium assumption for the modeling of surface tension forces. This model allows redistribution of surfactants at the surface. This was seen to have a large impact on the quantitative predictions from the models. In this work, simulations were restricted to time dependent axisymmetric weld pools, i.e. with a stationary heat source. Here, some recent 3D simulations of realistic weld pools are surveyed, (Do-Quang and Amberg, 2003; Do-Quang, 2004), including redistribution of surfactants and non-equilibrium at the interface.

2. Mathematical modeling

The fluid flow in the weld pool is mainly driven by forces due to surface tension gradients (Marangoni convection), but is also strongly influenced by electromagnetic forces and buoyancy, (Mundra and Debroy, 1993a, b; Oreper and Szekely, 1984). Arc pressure and aerodynamical drag forces arising from the shielding gas used in GTA welding to prevent oxidation have an impact on the welding process. Moreover, heat losses due to radiation and convection and solidification of the weld fusion zone as well as the modeling of the heat input from the arc present between electrode and workpieces have to be taken into account. The process is also highly influenced by the presence of surface active elements on the surface of the melt. In the case of stainless steel, sulfur and oxygen are known to be surface active.

A generic case for studying weld pool phenomena would consider a flat plate and an electric arc struck between an electrode above the surface and the plate. The molten weld pool develops directly beneath the electrode when the current is turned on and its shape and size is highly influenced by the heat and fluid flow in the molten zone. In what follows, we will assume that the workpiece is a large plate of a finite thickness.

The transport phenomena occurring inside the weld pool could be analyzed using the fundamental equations of continuity, momentum and energy, as presented in our previous study (Do-Quang and Amberg, 2003). In this paper, the surfactant transport equations are added. The fundamental equation of momentum is simplified according to the Boussinesq approximation by considering the liquid metal as an incompressible Boussinesq liquid, i.e.:

$$\nabla \cdot u = 0 \tag{1}$$

$$\frac{\partial u}{\partial t} + u \cdot \nabla u = -\frac{1}{\rho}\nabla p + \nu \nabla^2 u + S \tag{2}$$

$$\frac{\partial T}{\partial t} + u \cdot \nabla T = -\alpha \nabla^2 T + \frac{L^*}{\rho C_p}\,\frac{\partial \chi}{\partial t} \tag{3}$$

Here, u is the fluid velocity, p is the pressure and T is temperature. S is a source term, which includes the effect of Lorentz forces, possible flow resistance in a two-phase region, etc. (Do-Quang and Amberg, 2003):

$$S_x = \frac{1}{\rho}(\mathbf{J} \times \mathbf{B})_x + \frac{\nu}{H(\chi)}\,\chi u_x \tag{4}$$

$$S_y = \frac{1}{\rho}(\mathbf{J} \times \mathbf{B})_y + \frac{\nu}{H(\chi)}\,\chi u_y \tag{5}$$

$$S_z = \frac{1}{\rho}(\mathbf{J} \times \mathbf{B})_z + \frac{\nu}{H(\chi)}\,\chi u_z + g\beta(T - T_{\text{ref}}) \tag{6}$$

The $\mathbf{J} \times \mathbf{B}$ terms are the Lorentz force components in the respective directions, where the solenoidal vectors **J** and **B** are the current density vector and magnetic flux vector. Those are calculated by solving the Maxwell's equations of the electromagnetic field in the domain of the workpiece. If the effect of fluid motion on the electromagnetic field is neglected, the Lorentz forces are assumed constant and they are computed numerically and included to the system equations as a known body force.

Melting and solidification is assumed to take place at a fixed melting temperature. This is incorporated as a very simplified mushy zone model, with a very narrow freezing range, using the solid fraction χ. The function H(χ) denotes the permeability in the mush, as a function of solid fraction.

The surface tension gradient enters as a boundary condition for shear stress on the free surface (index s indicates a surface gradient operator):

$$\mu((\nabla u) + (\nabla u)^T) \cdot n = \nabla_s \gamma = \frac{\partial \gamma}{\partial T} \cdot \nabla_s T \tag{7}$$

As shown by Stebe and Barths-Biesel (1995), the surfactant appears subdivided into two phases: a bulk phase, with a concentration per volume C, and a surface phase, with a concentration per area Γ. The surface phase, supposed to be a monolayer, directly modifies the interfacial surface tension by the surfactant equation of state, $\gamma = f(\Gamma)$. In general, the equation of state is a non-linear function where increasing Γ reduces γ. The redistribution of the surfactant in the bulk liquid is due to convection and diffusion as:

$$\frac{\partial C}{\partial t} + u \cdot \nabla C = D_m \nabla^2 C \tag{8}$$

Here, D_m is the bulk diffusion coefficient of the surfactant in the liquid material. The concentration of surfactant on the free surface Γ is determined by surface convection and diffusion:

$$\frac{\partial \Gamma}{\partial t} + \nabla_s \cdot (u_s \Gamma) = D_i \nabla_s^2 \Gamma + j_n \tag{9}$$

The mass flux j_n to the interface occurs in a two-step serial process. The first step involves diffusion of surfactant from bulk layer. In this case j_n is provided by Fick's law, according to:

$$j_n = -D_m n \cdot \nabla C \tag{10}$$

The second step involves an adsorption to the free surface and can be computed by using the Langmuir adsorption kinetics theory, (Stebe and Barths-Biesel, 1995; Chen and Stebe, 1997):

$$j_n = k_\beta C_S(\Gamma_{\text{inf}} - \Gamma) - k_\alpha \Gamma \tag{11}$$

Here, Γ_{inf} is the upper bound on the surfactant concentration for monolayer adsorption. The adsorption rate, the first term on the right hand side, is assumed to be first order in bulk concentration immediately adjacent to the surface, C_s, and proportional to the deviation from a surface concentration corresponding to a completely covered surface. The desorption rate, the second term on the right hand side, is proportional to the surface concentration Γ. This flux balance equation will be used as a Neumann boundary condition expressing the diffusion of surfactant from the bulk layer when solving the bulk transport equation (5). On the other hand, the mass flux in the surface transport equation (6) will be associated with the adsorption-desorption flux in equation (8).

At equilibrium, the bulk flux in equation (8) is zero, and the equilibrium adsorption isotherm, corresponding to an equilibrium value Γ_{eq} of the surface concentration is obtained as:

$$\Gamma_{eq} = \Gamma_{inf} \frac{k_{\alpha\beta} C_S}{1 + k_{\alpha\beta} C_S} \tag{12}$$

Here, the adsorption number $k_{\alpha\beta} = k_\alpha / k_\beta$, the ratio of the characteristic rate of adsorption to desorption. The relation between equilibrium surface tension γ_{eq}, to equilibrium surface concentration Γ_{eq}, is determined by Gibbs thermodynamic relationship:

$$\mathrm{d}\gamma = -RT\Gamma \mathrm{d}(\ln C_S) \tag{13}$$

Here, R is the universal gas constant and T is the temperature. From equations (9) and (10), the Langmuir equation of state is obtained:

$$\gamma = \gamma_{eq} - RT \frac{\Gamma_{inf} - \Gamma}{\Gamma_{inf} - \Gamma_{eq}} \tag{14}$$

where γ_{eq} is the surface tension of pure melt at the melting point

At thermodynamical equilibrium, the coefficient of surface tension depends on temperature and the activity of surfactants in the base material (Sahoo *et al.*, 1988):

$$\frac{\partial \gamma}{\partial T} = -A_2 - R\Gamma_{inf} \ln(1 + K_{seg} a_i) - \frac{K_{seg} a_i}{1 + K_{seg} a_i} \frac{\Gamma_{inf} \Delta H^0}{T} \tag{15}$$

where a_i is the activity of the surface active species i, A_2 is the constant $-\partial\gamma\partial T$ for the pure material, and ΔH^0 is the standard heat of adsorption. The equilibrium constant for segregation K_{seg} is obtainable from equation (13), where k_l is a constant related to the entropy of segregation:

$$K_{seg} = k_l e^{-\frac{\Delta H^0}{RT}} \tag{16}$$

The activity of surfactants a_i can be expressed in terms of surface concentration Γ (Winkler *et al.*, 2000) as:

$$a_i = \frac{k_\alpha}{k_\beta} \frac{\Gamma}{\Gamma_{inf} - \Gamma} C_f \tag{17}$$

where C_f is a conversion factor from (mol m^{-3}), the unit of the bulk concentration, to (wt%), the unit of the surfactant activity.

3. Results and discussion

A pure liquid will usually exhibit a surface tension that decreases with temperature. In a welding situation, such as sketched in the left panel of Figure 1, this will cause a convection in the melt that is directed away from the hottest point on the surface, towards the rim of the pool. In welding, this is undesired since hot melt will be transported radially outwards, and a wide and shallow pool is created. However, in the presence of some surface active elements, in steel typically sulfur or oxygen, surface tension may instead increase with increasing temperature. The flow pattern is then reversed, in that the point of highest surface tension is thus the hottest point, and fluid on the surface is pulled radially inwards, and then deflected downwards, see the right panel in Figure 1. This will create a deep narrow pool, which will penetrate the material more easily (Figure 2).

As an example Figure 3 shows results from a simulation of a weld pool using parameter values for a stainless steel with very low-sulfur content (0.0005 wt%). The lower left panel shows the plate cut along the vertical symmetry plane. Only about the upper-third of the plate thickness is shown. The heat source is moving to the left in the figure, at 10 mm/s. At this very low-sulfur content the shape of the weld pool is not beneficial, compare the left panel in Figure 1. The rather complicated shape is best understood by looking at the top right panel in Figure 3. This shows the cross section along the symmetry plane for the case of a stationary heat source. The radius and

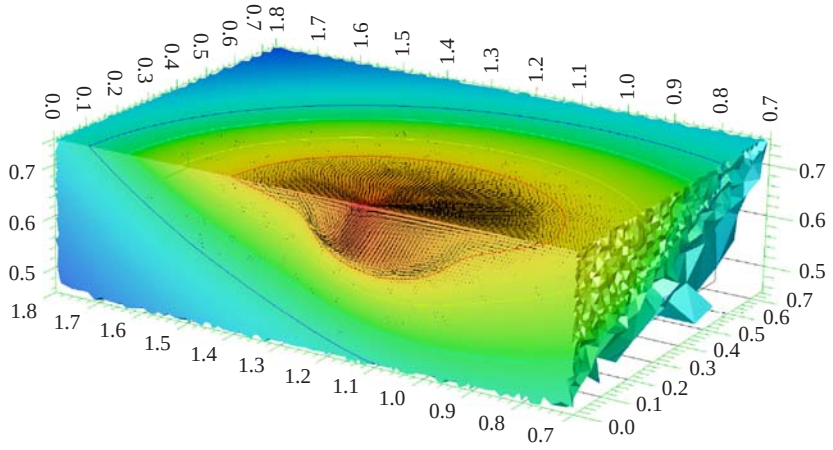

Figure 1.
Example of weld pool shape in a steel with higher sulfur content (0.0027 wt%), weld speed 9 mm/s

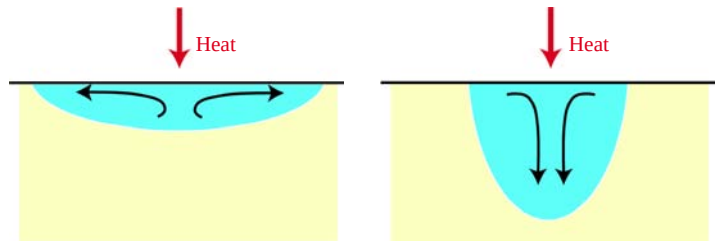

Figure 2.
Flow patterns in welding

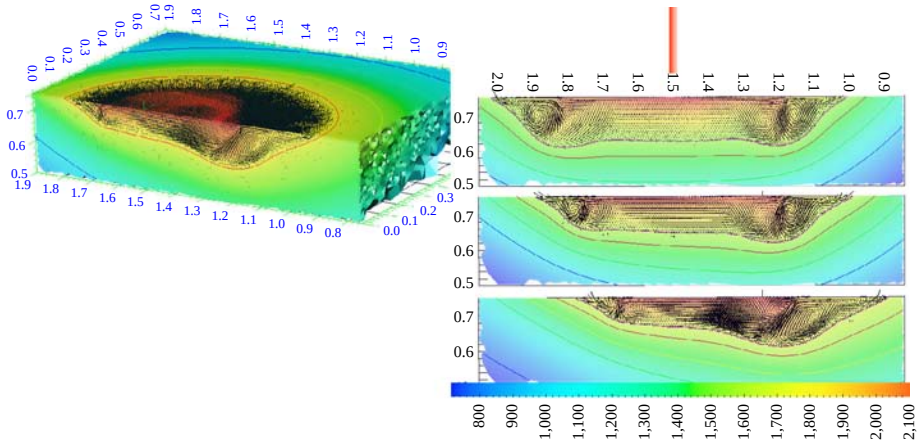

Notes: Weld current 100A, voltage 10.6V. Left panel: heat source moving to the left at 10 mm/s. In the right top, middle and bottom panels, the vertical arrow indicates the position of the heat source, moving to the left at speeds 0, 5 and 10 mm/s, respectively. In all panels the color indicates the temperature

Figure 3.
Example of weld pool shapes in a steel with low-sulfur content (0.0005 wt%)

depth at the center are about 2.1 and 0.57 mm, respectively, (scale in figure is normalized). The flow field is indicated inside the melt pool, and iotherms are drawn outside. The velocity magnitude is in the order of 0.1 m/s.

For this low-sulfur steel, the surface tension is a decreasing function of temperature over most of the surface, causing the strong radial outflow along the surface. At a certain radial distance, the hot surface flow is deflected downwards, to cause a localized depression at the weld pool bottom. In this axisymmetric shape, this means that a groove is formed near the rim of the pool. The maximal depth of the pool is thus obtained at a certain finite distance from the heat source. This rather unexpected behavior is due to a local maximum of the surface tension, that is obtained at a temperature rather close to the melting temperature, and thus rather close to the rim, for this low-sulfur steel. This local maximum in surface tension means that the Marangoni forces will cause the flow field to have a converging stagnation point at the surface there.

In the middle and bottom right panels in Figure 3, the heat source speed is increased to 5 and 10 mm/s, respectively. The motion is to the left in the Figure. It is seen that, as the speed increases, the leading side of the peripheral groove is weakened, while more heat is accumulated at the rear, causing a relative increase in depth there. The overall lateral size of the pool remains approximately the same, but the whole pattern is displaced towards the rear. As the axial symmetry is broken the flow pattern becomes increasingly complex.

In the presence of more surfactants, the flow pattern will be reversed. Figure 1, at approximately the same parameter setting as above, but with a sulfur content of 0.0027 wt%, the surface tension will increase with temperature in the relevant temperature range, and will be maximal at the hottest point, right below the heat source. The flow pattern will then be that indicated in the right panel in Figure 1, resulting in this particular case in a deeper pool.

Having observed the importance of minute concentrations of surfactants, it is clear that detailed modeling of surface tension is crucial for accurate results. In the past,

equilibrium models have been used that assume that the surfactant concentration at the surface is in perfect equilibrium. However, in the presence of a rapid fluid flow there is a coupling between the flow field and the surface tension. Consider a stagnation point flow on the surface, where fluid rises to, and spreads out along the surface, see the left panel in Figure 4. The surface is thus stretched and the local surface concentration of surfactant would tend to decrease. Since, the surface tension increases with decreasing surfactant concentration, the surface tension increases, and thus a restoring force appears. In the case of a converging stagnation point, see the right panel in Figure 4, the local concentration increases, causing a decreased surface tension and, again a restoring force. This effect is sometimes called surface "elasticity" (Chen and Stebe, 1997). Non-equilibrium effects would thus tend to reduce the expected flow velocities. In the present simulations this was modeled using equation (6) to compute the surface concentration Γ as an independent variable. In previous studies, (Winkler *et al.*, 2000), we have found it to be necessary to include these effects in order to predict pool depth and width with accuracy. Good agreement was obtained for a variety of experimental conditions.

Figure 5 shows the computed surface concentration of sulfur together with the flow field, as viewed from above, for a case with a moving electrode (weld speed $U_s = 1.6$ mm/s, $I = 100$ A, $U = 10.2$ V, low-sulfur concentration). The left panel shows isotherms and flow field, the right panel surface concentration. The motion of the electrode is upwards in the figure, causing an egg shape of the weld pool, with a circular leading side, and a somewhat elongated trailing side. The heat source is located at $x = y = 0$, in the upper part of the figures. As in the case shown in Figure 3, the sulfur concentration is low, so that over most of the surface the surface tension is decreasing with temperature. The corresponding flow pattern on the free surface is directed outward, away from the heat source. At this low-welding speed, the axismymmetric pool (cf top right panel in Figure 3) is only modestly distorted. In the rear part of the pool however, there is a distinct stagnation line separating a trailing region where flow velocities are smaller, and actually are reversed. The stagnation line in the velocity clearly coincides with a band of increased sulfur concentration, as shown in the right panel. As expected, sulfur is accumulated at a converging stagnation line. Conversely, the sulfur concentration is decreased over the central part where the surface flow is diverging.

4. Conclusions

Some basic concepts in the modeling of flow in a weldpool are reviewed. The mathematical models for a convecting melt, with a detailed model for the surface tension and the Marangoni stress in the presence of surfactants is presented. The effect of the sign of the Marangoni coefficient $\partial\gamma/\partial T$ on the flow pattern, and thus, via melting and freezing,

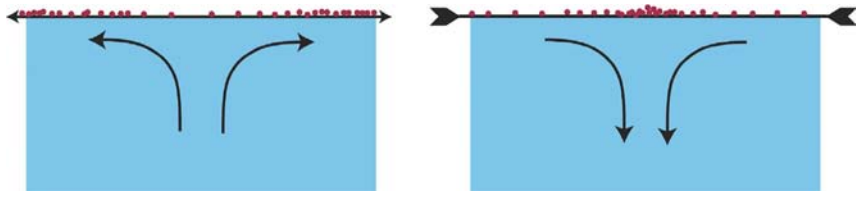

Figure 4.
Sketch of the mechanism of surface elasticity

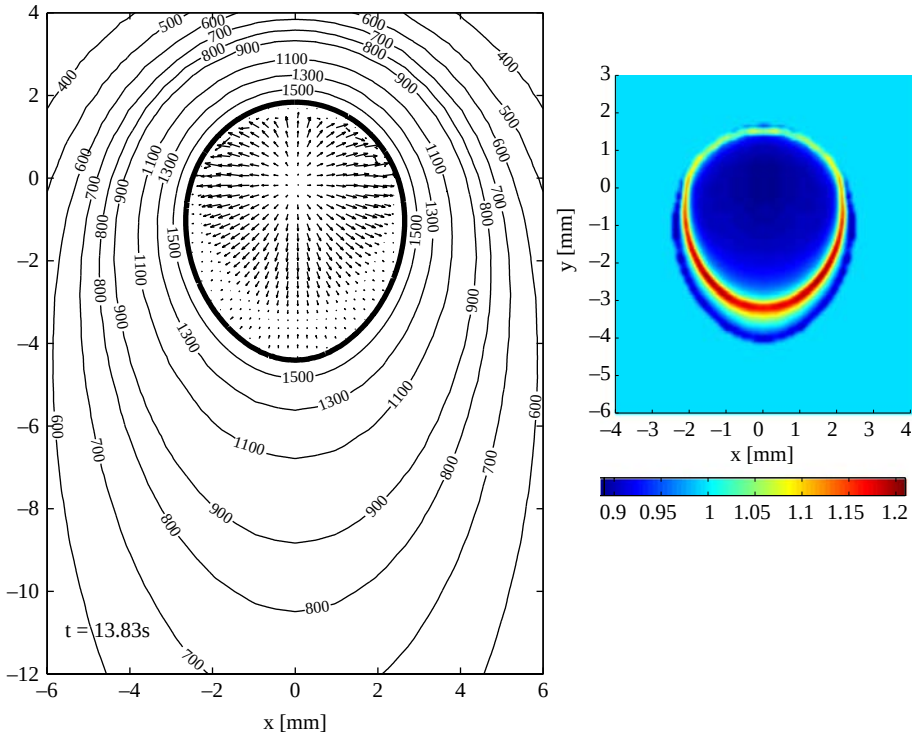

Figure 5.
Weld viewed from above, showing isotherms and flow field at the surface (left panel) and surface concentration of sulfur (right panel)

Notes: Weld speed U_s = 1.6 mm/s; I = 100A; U = 10.2V, low sulfur concentration

on the shape of the weld pool is discussed. It is seen that it is beneficial to have surfactants present at the pool surface, in order to have good penetration. Results from a refined surface tension model that accounts for non-equilibrium redistribution of surfactants are presented. It is seen that the surfactant concentration is significantly modified by the fluid flow. Thereby the effective surface tension and the Marangoni stresses are altered, and the redistribution of surfactants will affect the penetration depth of the weld pool.

References

Cerjak, H. (2001), *Mathematical Modelling of Weld Phenomena 6*, The Institute of Materials, London.

Chen, J. and Stebe, K.J. (1997), "Surfactant-induced retardation of the thermocapillary migration of a droplet", *J. Fluid Mech.*, Vol. 340, pp. 35-59.

David, S.A. and Vitek, J.M. (Eds) (1993), *International Trends in Welding Science and Technology*, ASM International, Materials Park, OH.

Debroy, T. and David, S.A. (1995), "Physical processes in fusion welding", *Review of Modern Physics*, Vol. 67, pp. 85-112.

Do-Quang, M. (2004), "Melt convection in welding and crystal growth", TRITA-MEK 2004:15, doctoral thesis, Department of Mechanics, KTH, Stockholm.

Do-Quang, M. and Amberg, G. (2003), "Modelling of time-dependent 3D weld pool flow", *Math. Modeling of Weld Phenomena, 7*, The Institute of Materials, London.

McNallan, M.J. and Debroy, T. (1991), "Effect of temperature and composition on surface tension in Fe-Ni-Cr alloys containing sulfur", *Metall. Trans.*, Vol. 22B, pp. 557-60.

Mundra, K. and Debroy, T. (1993a), "Calculation of weld metal composition change in high-power conduction mode carbon dioxide laser-welded stainless steels", *Metallurgical Transactions B*, Vol. 24B, pp. 145-55.

Mundra, K. and Debroy, T. (1993b), "Toward understanding alloying element vaporization during laser beam welding of stainless steel", *Welding Journal Research Supplement*, Vol. 72, pp. 1-9.

Oreper, G.M. and Szekely, J. (1984), "Heat-flow and fluid-flow phenomena in weld pools", *J. Fluid Mech.*, Vol. 147, pp. 53-79.

Sahoo, P., Debroy, T. and Mcnallan, M.J. (1988), "Surface tension of binary metal – surface active solute systems under conditions relevant to welding metallurgy", *Metall. Trans.*, Vol. 19B, pp. 483-91.

Stebe, K.J. and Barths-Biesel, D. (1995), "Marangoni effects of adsorption-desorption controlled surfactants on the leading end of an infinitely long bubble in a capillary", *J. Fluid Mech.*, Vol. 286, pp. 25-48.

Winkler, C., Amberg, G., Inoue, H., Koseki, T. and Fuji, M. (2000), "The effect of surfactant redistribution on the weld pool shape during GTA-welding", *Sci. Tech. Weld. Join.*, Vol. 5, pp. 1-13.

Corresponding author
Gustav Amberg can be contacted at: gustava@mech.kth.se